Ion conduction in substates of the batrachotoxin-modified Na^+ channel from toad skeletal muscle

David Naranjo and Ramón Latorre

Departamento de Biología, Facultad de Ciencias, Universidad de Chile; and Centro de Estudios Científicos de Santiago, Casilla 16443, Santiago 9, Chile

ABSTRACT Batrachotoxin-modified Na^+ channels from toad muscle were inserted into planar lipid bilayers composed of neutral phospholipids. Single-channel conductances were measured for $[Na^+]$ ranging between 0.4 mM and 3 M. When membrane preparations were made in the absence of protease inhibitors, two open conductance states were identified: a fully open state (16.6 pS in 200 mM symmetrical NaCl) and a substate that was 71% of the full conductance. The substate was predominant at $[Na^+] > 65$ mM, whereas the presence of the fully open state was predominant at $[Na^+] < 15$ mM. Addition of protease inhibitors during membrane preparation stabilized the fully open state over the full range of $[Na^+]$ studied. In symmetrical Na^+ solutions and in biionic conditions, the ratio of amplitudes remained constant and the two open states exhibited the same permeability ratios of P_{Li}/P_{Na} and P_{Cs}/P_{Na}. The current–voltage relations for both states showed inward rectification only at $[Na^+] < 10$ mM, suggesting the presence of asymmetric negative charge densities at both channel entrances, with higher charge density in the external side. An energy barrier profile that includes double ion occupancy and asymmetric charge densities at the channel entrances was required to fit the conductance–$[Na^+]$ relations and to account for the rectification seen at low $[Na^+]$. Energy barrier profiles differing only in the energy peaks can give account of the differences between both conductance states. Estimation of the surface charge density at the channel entrances is very dependent on the ion occupancy used and the range of $[Na^+]$ tested. Independent evidence for the existence of a charged external vestibule was obtained at low external $[Na^+]$ by identical reduction of the outward current induced by micromolar additions of Mg^{2+} and Ba^{2+}.

INTRODUCTION

Many types of ionic channels exhibit more than one conductance state (for a review see Fox, 1987; Meves and Nagy, 1989). The structural bases underlying the transitions between different conductance states are unknown; however, in a few cases it has been possible to induce subconductance states. For example, micromolar addition of either Cs^+ or Rb^+ to the external side of the inward rectifier K^+ channel induces the appearance of substates that are one- or two-thirds of the main conductance (Matsuda et al., 1989). To explain these findings, it has been proposed that the channel consists of three parallel conducting units each blocked independently by Cs^+ or Rb^+. A similar model was proposed for the Torpedo Cl^- channel in which DIDS can block independently one of two parallel pores (Miller, 1982).

Subconductance states have been observed for the unmodified Na^+ channels from cardiac and skeletal muscle (Cachelin et al., 1983; Patlak, 1988). However, their contribution to the total Na^+ current is small due to infrequent occurrence and brief openings. Nevertheless, the study of these subconductance states may provide useful insights into the channel permeation structure. To prolong Na^+ channel openings, treatment by pharmacological agents that remove or delay the inactivation process in Na^+ channels facilitate the study of conductance states (Green et al., 1987; Recio-Pinto et al., 1987; Patlak, 1988; Nilius et al., 1989; Schreibmayer et al., 1989; Levinson et al., 1990; Schild et al., 1991).

Batrachotoxin (BTX) is an alkaloid that eliminates both fast and slow inactivation of Na^+ channels, making possible steady-state recording of Na^+ currents (Khodorov, 1985). This toxin has proven useful to study isolated channels in planar lipid bilayers in which control of both the ionic and lipid environment surrounding the channel protein is possible (see Miller, 1986; Latorre, 1986). BTX-modified Na^+ channels in planar lipid bilayers exhibit subconductance states when the ionic strength is modified. For example, Green et al. (1987) showed a "flickery" substate that becomes predominant at $[Na^+] < 20$ mM. Similar results are reported by Recio-Pinto et al. (1987).

In this study we compare the "fully open" and a subconductance state of the BTX-modified Na^+ channel from toad skeletal muscle incorporated into a planar lipid bilayers. We show that under a wide variety of ionic conditions the ratio between the conductances of both states remains constant, suggesting that both states share the same mechanism of ion transport. Part of this work has been presented previously in abstract form (Naranjo et al., 1989, 1990).

MATERIALS AND METHODS

Planar bilayers and channel incorporation

Skeletal muscle membrane preparations from the Chilean toad *Caudiverbera caudiverbera* were performed as previously described (Hidalgo

Address correspondence to Dr. David Naranjo, Department of Neurobiology and Behavior, State University of New York at Stony Brook, Stony Brook, New York 11794-5230.

This article is based in part on a thesis submitted by D. Naranjo in partial fulfillment of the requirements for the Ph.D. in Biology at Universidad de Chile.

0006-3495/93/04/1038/13 $2.00

et al., 1986). When protease inhibitors were used, the homogenization step was done in the presence of 1 mM phenylmethylsulfonyl fluoride, 0.4 μg/ml leupeptin, 0.4 μg/ml pepstatin, and 0.4 mM benzamidine. Membrane suspensions (1–4 mg protein/ml) were stored as 30-μl portions at −80°C.

Solutions used for bilayers containing brain phosphatidylethanolamine (Avanti Polar Lipids, Inc., Birmingham, AL) dissolved in *n*-decane at a final concentration of 10 mg/ml. Planar lipid bilayers were formed across 300-μm holes made in 17-μm-thick Teflon partitions (Cecchi et al., 1986). During bilayer formation, the capacitance was monitored until a stable value of 100–400 pF was reached. Then, BTX (gift from Dr. John Daly, NIH, Bethesda, MD) was added to the aqueous solution to a final concentration of 100 nM. Single BTX-modified Na^+ channels were transferred to the planar bilayer using the "fusion method" (Krueger et al., 1983). To facilitate fusion, a NaCl osmotic gradient was used with the highest concentration corresponding to the side where the vesicles were added (*cis* side). Sodium channels were recognized by their selectivity, voltage dependence, and their sensitivity to tetrodotoxin (TTX; Calbiochem Corp., La Jolla, CA) and decarbamoylsaxitoxin (dc-STX; gift from Dr. Edward Moczydlowski, Yale University School of Medicine). Channels inserted ~60% of the time with the TTX receptor side facing the *trans* aqueous chamber. After channel incorporation, the gradient was usually dissipated, adding NaCl to the *trans* side from a concentrated stock solution. When the channel conductance was measured at low $[Na^+]$, channels were incorporated in the presence of a 200 mM NaCl/5 mM MOPS-NaOH, pH 7.0, or a 200 mM NaCl/1 mM MOPS-NaOH gradient. After channel incorporation, the gradient was dissipated by perfusing the high-concentration side with 10 times the volume of the chamber of either 5 mM MOPS-NaOH or 1 mM MOPS-NaOH buffer. Sodium concentration was incrementally increased by adding aliquots of a stock NaCl solution to both sides of the chamber. At 5 mM MOPS-NaOH and 1 mM MOPS-NaOH buffer, determination of $[Na^+]$ by atomic absorption spectrophotometry (360; Perkin-Elmer Corp., Norwalk, CT), gave values of 2.2 mM (n = 3) and 0.4 mM (n = 2), respectively.

Electrical measurements and data analysis

The current passing through the membrane was measured with a two-electrode voltage clamp (Behrens et al., 1989). Single-channel currents were stored in digital format on video tape for subsequent analysis of channel conductance. Current amplitudes were determined by either measuring the peak current from the amplitude histograms or by measuring single-channel current amplitude from chart recordings. With the histogram method and filtering to 8 Hz (−3 dB), it was possible to resolve differences of 0.05 pA in channel current amplitudes (see Fig. 4). Single-channel conductances were determined from linear regression of the current over the range of voltages between ±30 mV.

Barrier model

A three-barrier, two-well, double-occupancy channel model was used to fit the current–voltage relations in symmetrical aqueous solutions, the conductance-$[Na^+]$ data, and the current–voltage curves obtained in biionic conditions (Alvarez et al., 1992). Single- or multiion occupancy for Na^+ was modeled by changing the amount of electrostatic repulsion ($A_{Na\text{-}Na}$) between the ions residing in the conduction system of the channel (for further details see Alvarez et al., 1992). Minimization of the summed squared differences between the experimental values and the values predicted by the barrier model was done using the Gauss–Newton algorithm (Alvarez et al., 1992). Well depth, peak height, the repulsion factor, and the surface charge density were variables. For simplicity, it was assumed that peaks and wells were symmetrically located at fixed position within the conduction system (see Fig. 6). To define the positions of the wells, by trial and error assays, we concluded that for every model studied the best fits were obtained when both wells were at 0.15 of the central barrier. Therefore, this last value was used in all calculations. Although it is true that the solutions obtained in this way may not be unique, as a general rule the fitting routine converged consistently to the parameters values shown in Tables 1–3.

The electrical field is the algebraic sum of the electrical fields induced by the applied voltage and the asymmetry of the surface potential. The electrical field drops linearly through the energy profile and is added point by point to compute the free energy of each peak and well. Thus, a change in either the applied voltage or in the ionic strength promotes a "tilt" in the potential energy profile for the permeant ion (MacKinnon et al., 1989; Villarroel, 1989; Alvarez et al., 1992). The fixed surface charge densities (σ in e/nm^2) at each vestibule are independent adjustable parameters. They are calculated according to the Gouy–Chapman double-layer theory (Grahame, 1947; McLaughlin, 1977); thus, they represent charged planar surfaces. The surface potential, Φ_s, at each vestibule is related to the bulk, C_0, concentration of monovalent cations and σ through the relation:

$$\Phi_s = (2RT/F)\ \text{arcsinh}\ (1.36\sigma/\sqrt{C_0}). \qquad (1)$$

The calculations using this model are aimed at determining whether this type of energy profile adequately describes the current–voltage relations obtained in the different experimental conditions. They are further useful in obtaining estimates of the vestibule charge density at very low ion concentrations. It is clear that more complicated models that do not assume equivalence of the three peak and well energies (a simplifying assumption made to reduce the number of parameter in the model) would fit the data as well. However, it is important to bear in mind that to fit simultaneously the I-V relations and the channel conductance versus $[Na^+]$ relations, independently of the number of parameters that are allowed to vary, the model needs to consider a charged pore.

Ion channel blockade and surface charge

The open channel current obtained in the presence of a blocking divalent cation, I, was fit to the following relation (Smith-Maxwell and Begenisich, 1987; MacKinnon et al., 1989),

$$I/I_0 = K_d/(C(\Phi) + K_d), \qquad (2)$$

where I_0 is the current in the absence of the blocking ion, $C(\Phi)$ is the calculated blocking ion concentration at the channel entrances according to $C(\Phi) = C_0 \exp(-zF\Phi_s/RT)$. Since Eq. 1 is only valid for the case of symmetrical electrolytes, for mixtures of divalent and monovalent cations with monovalent anions, Φ_s was solved numerically from the Gouy–Chapman expression for mixed electrolytes (Grahame, 1947),

$$\sigma = \pm[2RT\epsilon_0\epsilon_w \textstyle\sum C_i(\exp(-z_i\Phi_s/RT) - 1)]^{1/2}, \qquad (3)$$

where ϵ_0 is the permittivity of the free space, ϵ_w is the dielectric constant of water (78.5 at 24°C), and C_i is the concentration of the species i (for further details see Latorre et al., 1992).

RESULTS

BTX-modified Na channels from toad muscle exhibit two open conductance states

Two open states of different amplitude were observed in lipid bilayers prepared from muscle membrane fractions. Both states were observed when membrane was prepared in absence of protease inhibitors (API preparations). In the presence of 100 nM BTX and 200 mM symmetric NaCl, BTX-modified Na^+ channels fluctuated between a fully closed state (Fig. 1 *A, broken line*) and either an intermediate open state (γ_2) with a conduc-

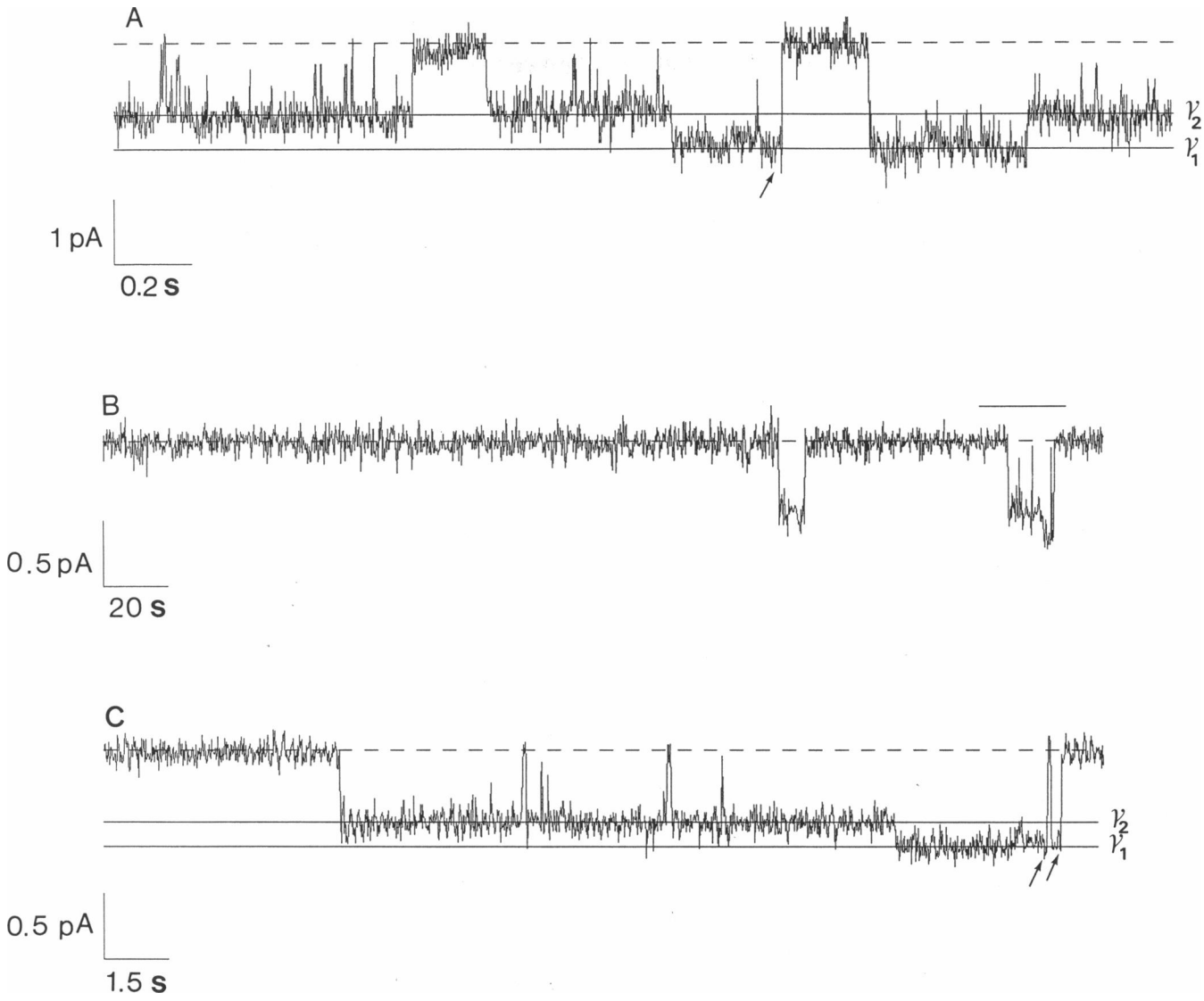

FIGURE 1 Characteristics of toad BTX-modified Na^+ channels. (*A*) Current fluctuations of a Na^+ channel recorded at −90 mV in symmetrical 200 mM NaCl, 5 mM MOPS-NaOH, pH 7.0. Broken lines indicate the closed-state current, and solid lines denote the current levels for the γ_1 (fully open) and γ_2 conductance states. Arrows mark direct transitions from γ_1 to the closed state. Filtering, 100 Hz. (*B*) Current fluctuations of a Na^+ channel obtained at −40 mV, in symmetrical 400 mM NaCl, 5 mM MOPS-NaOH, pH 7.0, and 33 nM external TTX. The horizontal line at the top of the record denotes the expanded region shown in *C*. Filtering, 50 Hz.

tance of 11.4 pS or a fully open state (γ_1) with a conductance of 16 pS. Both states are perfectly selective to Na^+ relative to Cl^- (data not shown), and tetrodotoxin induces long-lived closing events without affecting γ_1 and γ_2 states (Fig. 1 *B*). Both open states were also observed in the presence of dc-STX (Fig. 2 *A*). However, the mean blocked time induced by this toxin is briefer than those produced by TTX, permitting current amplitudes to be measured for a reasonable number of transitions.

The γ_1 and γ_2 open states are not two Na channels with different conductances; rather, they reflect the complex behavior of a single class of channel. This is based on the observation that only two open levels were observed, corresponding to γ_1 and γ_2. No openings to a level equivalent to $\gamma_1 + \gamma_2$ were observed as might be expected if the states represented openings by two independent channels (Fig. 1). A second line of evidence is that direct transitions to both open states were frequently observed. In the case of a two-channel membrane, simultaneous openings or closings by two independent channels are expected to be very infrequent (Fox, 1987).

Openings to γ_1 were favored in the $[Na^+]$ range of 0.4–15 mM (Fig. 2). By contrast, less frequent openings to the γ_1 level were observed at higher $[Na^+]$. At $[Na^+]$ >65 mM, γ_1 comprises only a very small fraction of the channel openings. From 46 bilayers containing either one or two channels, openings to the γ_1 state were observed in only two bilayers precluding measurement of

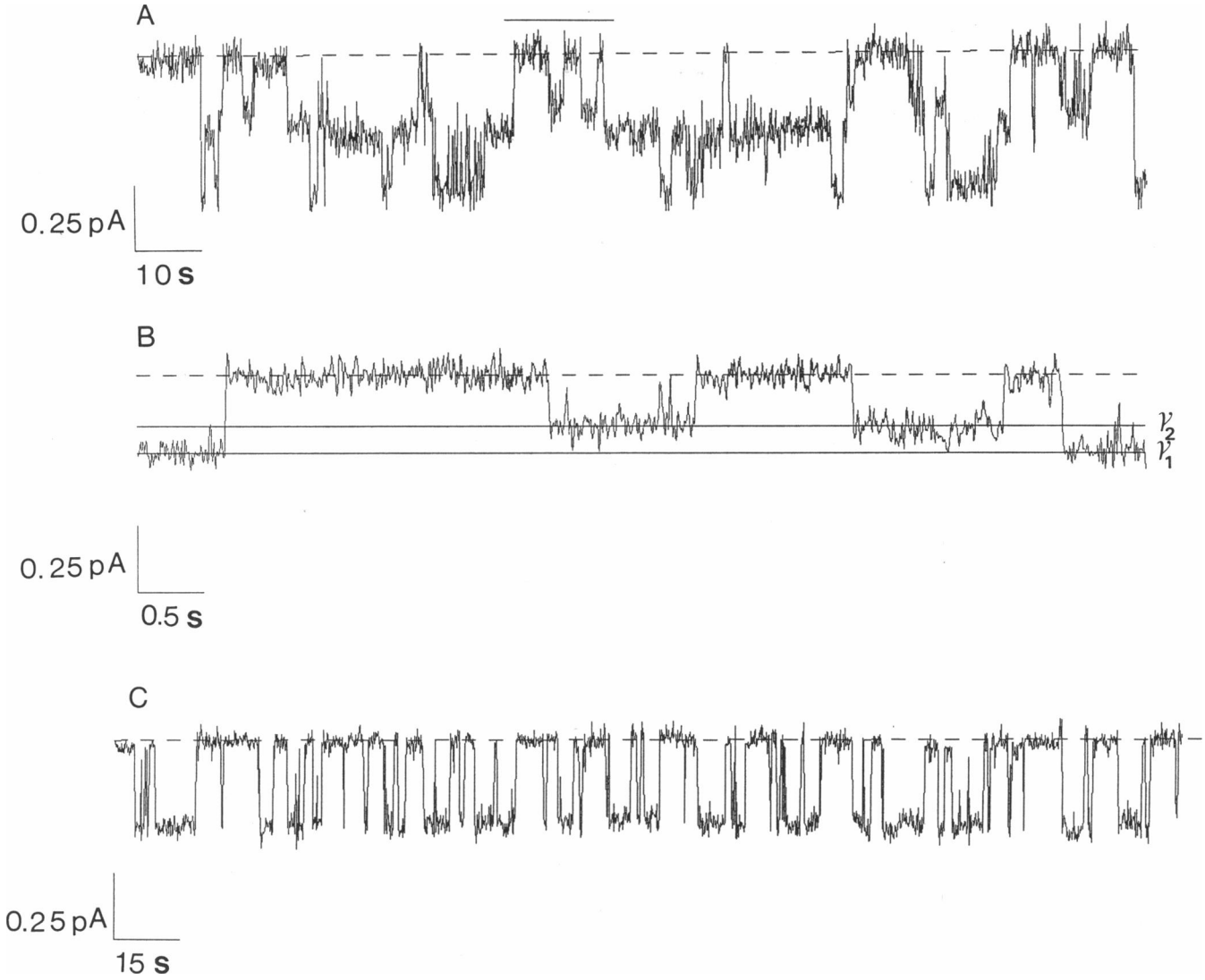

FIGURE 2 Low [Na^+] stabilize the fully open state. (*A*) Current traces taken at −35 mV in symmetrical 3 mM NaCl. dc-STX was added to the external side only to a final concentration of 0.6 nM. The short horizontal line on the top of the trace indicates the fragment of the record expanded in *B*. Broken lines indicate the closed state. Filtering, 10 Hz. (*C*) Current trace obtained in the same membrane as in *B*, but after 10 min of continuous recording, one of the two BTX-modified Na^+ channels present in the bilayer disappeared from the record. Note that during the ~4 min of recording the current trace showed in *C* lasted, only one conductance level can be appreciated corresponding to γ_1. Filtering, 5 Hz.

slope conductance at higher [Na^+]. The average conductance in symmetrical 200 mM NaCl for the γ_2 state of Na^+ channels from API membrane preparations was 11.4 ± 1.2 pS (n = 7 experiments).

Protease inhibitors stabilize the γ_1 conductance state

Different results were obtained when membrane preparations were made in the presence of protease inhibitors (PPI preparations). Fig. 3 *A* shows two consecutive current records of a bilayer containing three BTX-modified Na^+ channels from a PPI membrane preparation. As with the API preparation, transitions to two different open levels were observed. Given the ionic conditions under which these records were obtained (200 mM NaCl internal/5 mM MOPS-NaOH external), these transitions could be due to either a jump to a Na^+ channel substate or to the additional opening of a Cl^- channel. Fig. 3 *B* shows the current–voltage relationships for the fully open state and for the substate. Both conductances tend to negative reversal potentials, ruling out the possibility for a Cl^- channel transition. Therefore, the small conductance events correspond to a substate of a Na^+ channel. In PPI membrane preparations, transitions to γ_2 were observed in only 3 out of 55 bilayers containing one to three BTX-modified Na^+ channels precluding measurement of slope conductance. The average chan-

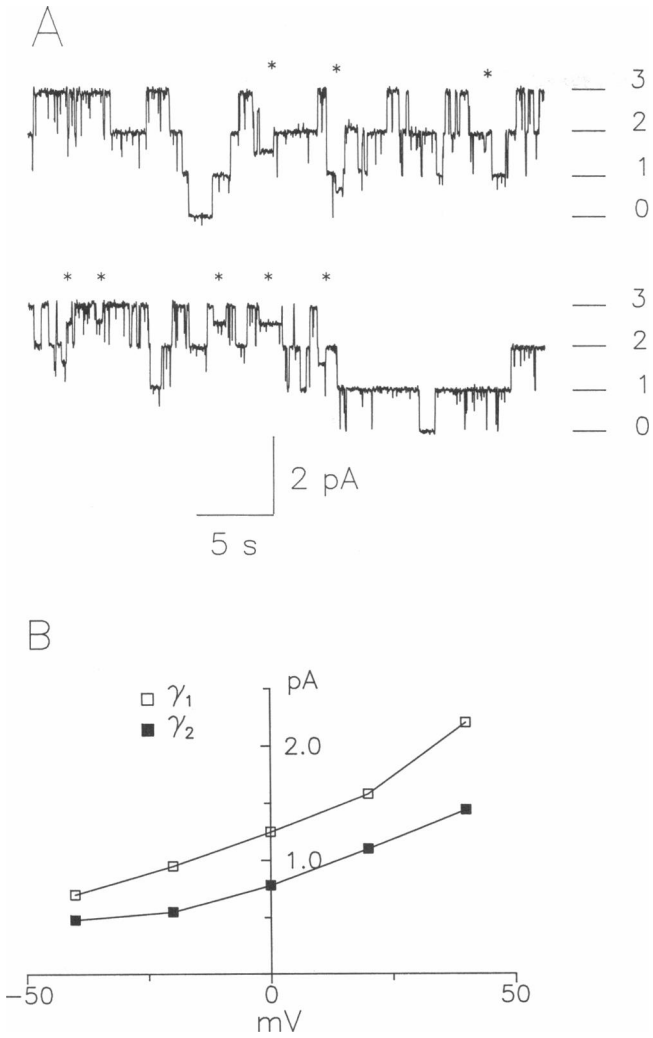

FIGURE 3 BTX-modified Na^+ channels from PPI membrane preparations also show a small conductance substate. (*A*) Channel current fluctuations at 0 mV in the presence of 200 mM NaCl, 5 mM MOPS-NaOH, pH 7, in the internal side and 5 mM MOPS-NaOH, pH 7, in the external side of the channel. The small horizontal lines at the right of the record indicate current levels corresponding to zero, one, two, or three channels open. Asterisks mark channel transitions from γ_1 to γ_2. Filtering, 20 Hz. (*B*) Current–voltage relationships for γ_1 and γ_2. Experimental conditions are as in *A*.

nel conductance in symmetrical 200 mM NaCl for γ_1 was 16.6 ± 1.5 pS (n = 5 experiments). This value for Na^+ channel conductance was 46% larger than that measured for γ_2 channels present in the API preparations.

Two findings indicate that the higher conductance states of both membrane preparations are identical, and therefore the lower conductance states of both preparations are indistinguishable. First, current–voltage relationships obtained at 2 mM for the higher conductance state of channels from API membranes and for the main conductance state of channels from PPI preparations are indistinguishable (see Fig. 5 *A*). Second, the ratio of currents between the main state and the substate of PPI preparations (Fig. 3) is 1.51, which is very similar to the conductance ratio γ_1/γ_2 = 1.47 obtained from API preparations (Fig. 1, *A* and *C*).

Channel conductance as a function of voltage and [NaCl]

At low [Na^+], it is possible to measure unitary currents for both conductance states using API membrane preparations. For this purpose, event amplitude histograms were constructed over a range of voltages (Fig. 4). This method resolved current differences of ~0.05 pA. The conductances for γ_1 and γ_2 measured in 3 mM Na^+ were 7.9 and 5.5 pS, respectively. These values, compared with 16.6 and 11.4 pS measured in 200 mM Na^+ for γ_1 and γ_2, represent only a twofold change in conductance for a 67-fold change in [Na^+].

Current–voltage relations for γ_1 and γ_2 were nearly linear over the range of potentials between ±45 mV (Fig. 5). The slope conductances for γ_1 obtained over this range were 7.3, 16.8, and 29 pS in 2, 200, and 3,000 mM Na^+, respectively. For γ_2, single-channel conductances under the same conditions were 5.5, 10.7, and 23.1 pS. Thus, the conductance ratio γ_1/γ_2 was nearly independent of [Na^+], measuring 1.33, 1.57, and 1.25 at 2, 200, and 3,000 mM Na^+, respectively.

However, at [Na^+] <10 mM and at potentials more positive than +45 mV, the current–voltage relations are sublinear. For γ_1, the current measured at −75 mV (Fig. 5 *A*; 2-mM Na^+ curve) was −0.62 pA and at +75 mV was 0.45 pA. This 0.17-pA difference in current is well above the 0.05-pA error of the current determination (see Materials and Methods and Fig. 4). For γ_2 (Fig. 5 *B*), the rectification amounts to a difference of 0.28 pA when the

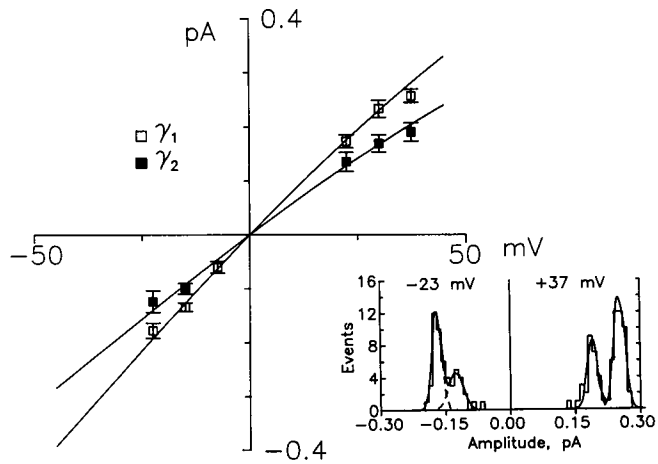

FIGURE 4 Current–voltage relations obtained from current amplitude histograms. The amplitude of 12–72 transitions lasting >100 ms were measured to build the histograms shown in the inset. The open and closed squares represent the mean of the corresponding Gaussian fitted to the current histograms. Solid lines are predicted curves obtained by using the charged-vestibule-3B2S model for γ_1 and γ_2 with the parameters given in Table 1 (two-ions and surface charge). API membrane preparation. Other experimental conditions are as in Fig. 2.

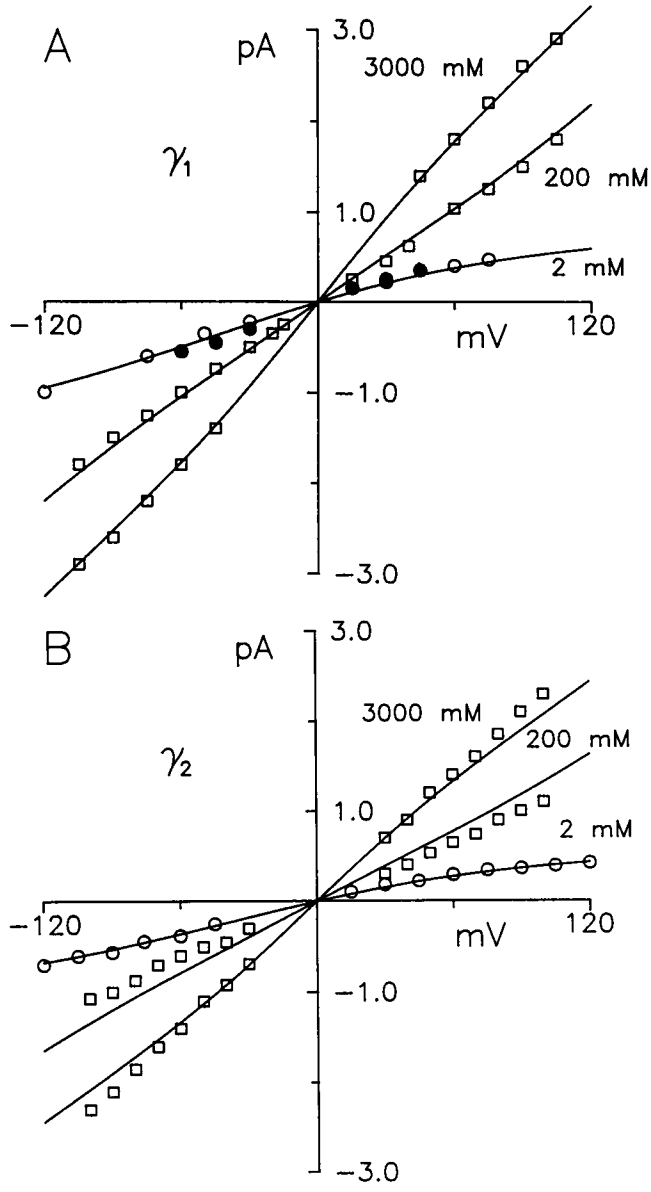

FIGURE 5 Current–voltage relations for BTX-modified Na^+ channels in symmetrical Na^+ solutions. (*A*) Open symbols correspond to data obtained using Na^+ channels contained in a API muscle membrane preparation (γ_1). The filled circles are the channel currents measured for γ_1 of a Na^+ channel from PPI muscle membrane preparation. (*B*) Open symbols are data taken for γ_2 of Na^+ channels contained in a API muscle membrane preparation. The solid lines are the predicted current–voltage relationships from the charged-vestibule-3B2S model.

current amplitudes were measured at ±120 mV. This inward rectification of the I-V relationship may indicate the presence of asymmetrically distributed negative charges at the two channel entrances (Dani and Eisenman, 1987; Villarroel, 1989; Latorre et al., 1992).

The conductance measured for γ_1 and γ_2 departs significantly from a simple Langmuir isotherm (Fig. 6). Moreover, conductances at low $[Na^+]$ are larger than expected for a channel that follows a Michaelis–Menten type of saturation. On the other hand, data for γ_1 and γ_2 show a biphasic shape, suggesting multiple ion occupancy (Naranjo et al., 1990; Ravindran et al., 1992). Thus, comparison of the ionic conduction properties of γ_1 and γ_2, required greater complexity than Michaelis–Menten conduction systems.

To account for excess of conductance at low $[Na^+]$, we considered the possibility of fixed negative charges at the channel entrances giving rise to a local electrostatic potential that would be expected to increase the local Na^+ concentration, thereby increasing channel conductance. When conductance versus $[Na^+]$ data were fitted by an energy barrier model that assumed both single-ion occupancy and charged vestibules, a poor correspondence was observed over the whole range of $[Na^+]$ (Fig. 6, *A* and *B, short dashed lines*). The double occupancy model

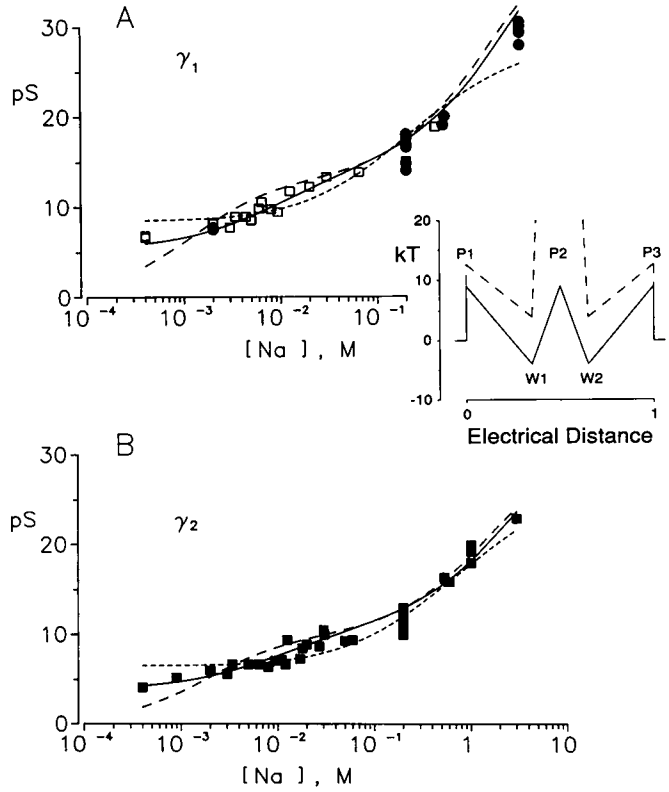

FIGURE 6 Conductance versus $[Na^+]$ relations for the conductance substates of the toad muscle BTX-modified Na^+ channel. (*A*) Conductance–$[Na^+]$ relation for γ_1. *Open squares,* Na^+ channel from API membrane preparation. *Closed circles,* Na^+ channel from PPI membrane preparation. (*B*) Conductance–$[Na^+]$ relation for γ_2. All data were obtained using Na^+ channels from API membrane preparations. The solid lines are the predicted curves obtained from the fit of all the current–voltage relations using the two-ion, charged-vestibule-3B2S model. The parameters used in the fittings of γ_1 and γ_2 are given in Table 1. The long dashed line is a fit to the data using a two-ion 3B2S model with uncharged vestibules, and the short dashed line is a fit to the data using a one-ion, charged-vestibule-3B2S model. *Inset,* a three-barrier two sites energy profile representing the total electrostatic energy to move one (*solid line*) or two ions (*broken line*) from the bulk solution into a model pore for the BTX-modified Na^+ channel. The profile shown correspond to the γ_1 substate. The profile does not include surface charge effects.

TABLE 1 **Energy parameters for the vestibules-3B2S energy barrier model under different ion occupancy and surface charge conditions**

	Peaks	Wells	$A_{Na\text{-}Na}$	σ_{in}	σ_{ex}	SMSQ
	kT	*kT*	*kT*	$-e/nm^2$	$-e/nm^2$	
γ_1						
One ion and surface charges	11.21 ± 0.75	−1.17 ± 0.84	∞	0.090 ± 0.007	0.124 ± 0.007	0.350
Two ions	7.00 ± 0.03	−6.10 ± 0.04	10.16 ± 0.33	—	—	0.105
Two ions and surface charges	8.96 ± 0.09	−4.04 ± 0.12	7.00 ± 0.53	0.022 ± 0.001	0.041 ± 0.002	0.091
γ_2						
One ion and surface charges	12.24 ± 0.05	−0.24 ± 0.06	∞	0.129 ± 0.005	0.157 ± 0.005	0.152
Two ions	7.69 ± 0.09	−5.69 ± 0.13	9.43 ± 0.91	—	—	0.947
Two ions and surface charges	9.30 ± 0.15	−3.98 ± 0.24	6.90 ± 1.70	0.022 ± 0.002	0.041 ± 0.004	0.073

$A_{Na\text{-}Na}$ is the electrostatic repulsion factor as defined in Materials and Methods. σ_{in} and σ_{ex} are the surface charge density in the internal and external vestibules, respectively. Data are means ± SD of the estimations. SMSQ is the summed squares of the differences between experimental data and the values predicted by the barrier model.

with neutral vestibule similar to that used by Ravindran et al. (1992) for rat muscle Na^+ channel gave a poor fit at low [Na^+] (*long dashed lines*). The best fit to the data was obtained using the 3B2S-charged-vestibule model that allowed double-ion occupancy (Table 1, *solid lines*). This model predicts limiting conductances at very low [Na^+] of 5.9 and 4.2 pS for γ_1 and γ_2, respectively.[1] The 3B2S-charged-vestibules model indicates (Table 1) that the main difference between the γ_1 and γ_2 states resides in the energy of peaks (peak energy difference = 0.40 kT) rather than in the wells (~0.1 kT) or in the surface charge density.

The I-V relations for γ_1 and γ_2 were best fitted when the surface charge density (σ) in the external vestibule was about twofold that of the inner vestibule (Table 1 and Fig. 5). Thus, the asymmetric transport properties that appear at low ion concentrations can be explained by a difference in the charge density of the vestibules.

Ion selectivity

Na^+ channels are highly permeable to Li^+ and relatively impermeant to Cs^+. If the difference in ion conduction between γ_1 and γ_2 resides only on differences in the energy barriers, then both conductances are predicted to show the same permeability ratios P_{Li}/P_{Na} and P_{Cs}/P_{Na}. By contrast, if the differences between γ_1 and γ_2 are due to a change in any other ion conduction parameters, we would expect a difference in those permeability ratios.

Under biionic conditions, with Na^+ in the external side of the membrane and Li^+ on the cytoplasmic side, the determined reversal potentials were 3.7 and 2.5 mV, respectively, giving $P_{Li}/P_{Na} = 0.80$ for γ_1 and 0.84 for γ_2 after appropriate compensation for junction potentials (Fig. 7 *A*). Despite the fact that the permeability ratios for Na^+ and Li^+ were close to unity, the chord conductances measured at ±75 mV differed by a factor of 1.8-fold. This finding suggests the presence of a site(s) in the Na^+ channel conduction system that binds Li^+ more tightly than Na^+. We were unable to determine γ_1 and γ_2 reversal potentials for Cs^+/Na^+ biionic case (Fig. 7 *B*). However, a fit to the data using the 3B2S-charge-vestibule model (*solid line*) predicts a $P_{Cs}/P_{Na} = 0.026$ for both γ_1 and γ_2. This latter value should be taken as an upper limit since even at positive potentials as high as 120 mV, currents are too small to be measured. These data suggest that the selectivity of the fully open and the substate of the toad muscle Na^+ channel is similar to the one found for other BTX-modified Na^+ (e.g., Behrens et al., 1989) and that both states discriminate ions roughly in the same manner.

Further evidence of the presence of fixed charges in the channel vestibules

The biphasic shape of the conductance versus [Na^+] curve, suggestive of multiion occupancy seen for both conductance states (Fig. 6), is in agreement with what has been observed for the BTX-modified Na^+ channel from rat skeletal muscle (Ravindran et al., 1992). However, these authors did not require the incorporation of surface charge effects to fit their data. Thus, additional experiments were performed to test for the presence of surface charges effects on the toad Na^+ channel.

Externally added impermeant cations to aqueous phases can provide independent evidence on the existence of fixed charges in the channel vestibules. In principle, the increase in ionic strength promoted by the im-

[1] At very low bulk [Na^+], the Gouy–Chapman theory predicts that the concentration of [Na^+] at the surface (C_0) becomes constant and independent of the bulk electrolyte concentration. In this low [Na^+] concentration limit, $C_0 = \sigma^2/2RT\epsilon_0\epsilon_s$ (McLaughlin, 1989; Latorre et al., 1992). To calculate the limiting conductances for the substates, σ was taken as 0.026 e/nm^2, and hence the limiting concentration C_0 is 6.32 mM. However, as pointed out by Green et al. (1987), the determination of the limiting conductance is affected by the series resistance due to the aqueous phases.

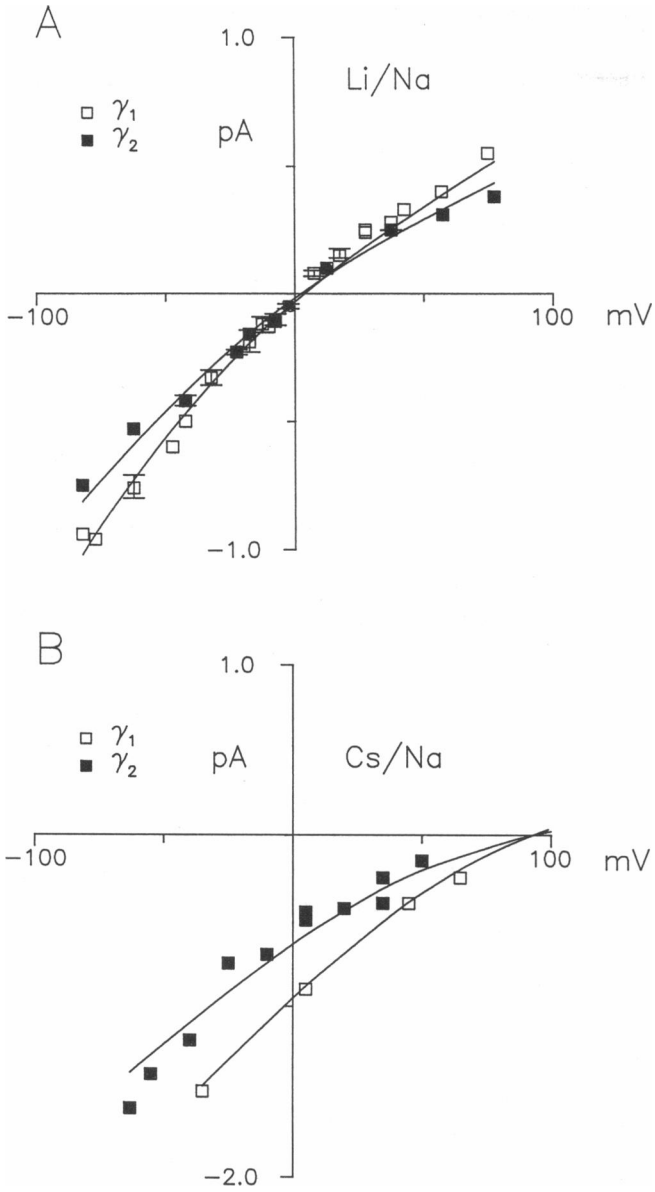

FIGURE 7 Ion selectivity of the channel. (*A*) BTX-modified Na^+ channels under biionic conditions with 200 mM LiCl, 5 mM MOPS-LiOH, pH 7, in the internal side and 200 mM NaCl, 5 mM MOPS-NaOH, pH 7, in the internal side of the channel. Symbols are data compiled from three experiments. Points and error bars refer to the mean ± SD. (*B*) BTX-modified Na^+ channels under biionic conditions with 200 mM CsCl, 5 mM MOPS-CsOH, pH 7, in the internal side and 200 mM NaCl, 5 mM MOPS-NaOH, pH 7, in the external side of the channel. γ_1, data compiled from a single experiment; γ_2, data compiled from two experiments. Standard errors of data points are smaller than symbols. The solid lines are predictions from the charged-vestibules 3B2S barrier profiles for Na^+, Li^+, and Cs^+. Energy parameters (γ_1) are (in units of kT): Li^+, peaks 9.11; wells −5.08; $A_{Li\text{-}Li}$ = 2.36; surface charge is as in Table 1. Cs^+, peaks 12.44; wells −1.64; $A_{Cs\text{-}Cs}$ = 0.64. For γ_2 the energy parameters are Li^+, peaks 9.58; wells −4.82; $A_{Li\text{-}Li}$ = 2.36 and Cs^+, peaks 12.97; wells −2.10; $A_{Cs\text{-}Cs}$ = 0.75.

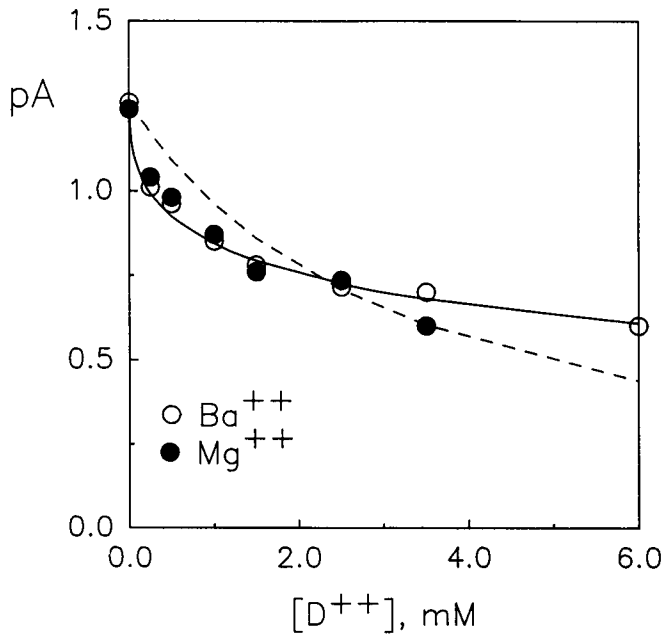

FIGURE 8 Reduction of outward current by external impermeant ions. The internal solution contained 200 mM NaCl, and the external solution was initially 5 mM MOPS-NaOH, pH 7.0. The applied voltage was 0 mV. $MgCl_2$ or $BaCl_2$ was added to the external solution to the indicated concentrations. The solid line corresponds to Eqs. 2 and 3, and the dashed line is the best fit to the data using Eq. 2 and assumes uncharged vestibules. The parameters describing the solid line are as follows: I_0 = 1.26 pA, K_d = 22 mM, and σ = −0.041 e/nm².

permeant cation would electrostatically induce a decrease in channel current because the screening of the surface charges. When impermeant cations Ba^{2+} or Mg^{2+} were added at varying concentration to the external aqueous solution, a decrease in the current was observed (Fig. 8). However, the decrease in channel conductance can also result from a fast blockade of the channel by the impermeant cation. In this case, a simple Langmuir isotherm for the open channel current versus the impermeant ion concentration curve is predicted (Eq. 2). However, the observed decrease in the current did not follow a Langmuir-type of behavior, showing at low impermeant ion concentrations a decrease larger than the one expected from a simple type of ion blockade mechanism (Fig. 8, *dashed line*). A reasonable fit to the data was obtained when it assumed the presence of a fixed charge near the permeation pathway (Fig. 8, *solid line*). The best fit was obtained by fixing σ in −0.041 e/nm² and leaving K_d as the only adjustable parameter yielding K_d = 22 mM. In the case of noncharged entrances, the K_d value converged to 3.2 mM. One of the consequences of the Gouy–Chapman theory is that charge screening only depends on the valence of the screening ion and not on the particular species used. This prediction is fulfilled by the fact that at the low concentrations, reduction of Na^+ currents was identical for both divalent cations. Thus, these results support the idea that surface charges in the channel entrances affect permeation through the Na^+ channel.

DISCUSSION

Multiple conductance states of the Na^+ channel

Our findings indicate that frog muscle Na^+ channels exhibit at least two open conductance states. The stability of either state depends on the $[Na^+]$ in the aqueous phases and the presence or absence of protease inhibitors during the process of membrane purification. Stabilization of a given open conductance state at a specific range of $[Na^+]$ has been reported by Green et al. (1987). They observed at $[Na^+]$ <500 mM, a "noisy" substate, with a conductance of ~50% of that of the fully open state. This noisy conductance state becomes more prominent as the $[Na^+]$ is reduced, such that the only open conductance state observed is at $[Na^+]$ <20 mM. Recio-Pinto et al. (1987) also noticed that the eel electroplax Na^+ channel shows a substate when $[Na^+]$ is 20 mM or lower.

The ratio of conductances γ_1/γ_2 remained constant over the very wide range of $[Na^+]$ studied and under the biionic Li/Na and Cs/Na conditions. This type of behavior has been found in several cationic and anionic channels (reviewed in Fox, 1987). At present, we do not know the structural changes responsible for the different conductance states. However, two simple models are compatible with the data. In one physical model, parallel conduction units share very similar ion conduction properties, like the mechanism proposed for the Torpedo electroplax chloride channel (Miller, 1982) and the cardiac inward rectifier (Matsuda et al., 1989). Although evidence supporting this structural model is not conclusive yet, this type of structure has been proposed for the Na^+ channel (Meves and Nagy, 1989; Schreibmayer et al., 1989). In a second physical model, the observed subconductance state could be due to a partial closure of the channel resulting from a segment of the protein that moves to partially occlude the pore (Fox, 1987). This segment could be loosened or released by proteases during the membrane preparation process.

Multiion conduction in BTX-modified Na^+ channels

Until recently, BTX-modified Na^+ channel data have been interpreted using single-ion conduction models (but see Begenisich and Cahalan, 1980*a, b;* Naranjo et al., 1990). Recently, Ravindran et al. (1992) found a biphasic relationship between unitary conductance and $[Na^+]$, suggestive of multiple occupancy. This biphasic behavior is apparent when electrostatic repulsion between ions occupying the channel exists (Hille and Schwarz, 1978). Thus, introduction of an electrostatic repulsion factor in a channel containing two identical sites along with double occupancy results in both sites saturating at different ion concentration. The biphasic shape of the conductance versus $[Na^+]$ data for γ_1 and γ_2 (Fig. 6) indicates that, for example, the dissociation constant (K_{app}) for the occupancy of the first site of γ_2 is 18 mM (−4 kT) and for the second site K_{app} is 47 M. At the latter concentration, a decrease in the conductance is expected because the rate of entry for the second ion exceeds the rate of exit. It is not possible to test this prediction due to the solubility limitations for sodium salts.

Origins of the surface charge heterogeneity between Na^+ channels

The conductance–$[Na^+]$ relation have been obtained for several different BTX-modified $[Na^+]$ channels incorporated into planar lipid bilayers (Table 2). Data from dog brain, eel electroplax, lobster peripheral nerve, and toad muscle Na^+ channels (Green et al., 1987; Recio-Pinto et al., 1987; Castillo et al., 1992; and present results) suggest the presence of charge at the channel entrances. On the other hand, rat brain, rat muscle, and squid optic nerve Na^+ channels (French et al., 1986; Moczydlowski et al., 1984; Behrens et al., 1989; Ravindran et al., 1992) show negligible surface charge density in the pore vestibules. These diverse estimates of surface charge density can have at least three different origins: (*a*) channel modification due to the biochemical treatment of the different membrane preparations similar to the protease effects observed in our study, (*b*) actual structural differences between channel types, and (*c*) small differences in charge exaggerated as a result of the use of single ion models to describe a multiion conduction system over narrow ranges of $[Na^+]$ (Ravindran et al., 1992). Although we cannot evaluate the effect of alternative *a*, in the two following sections we present arguments that support *b* and *c*.

Heterogeneity due to actual differences in Na^+ channels charge density

We found that it is necessary to invoke surface charge effects to account for both, the observed conductance (Fig. 6) and channel current rectification, seen at low $[Na^+]$ (Fig. 5). Furthermore, because ion valence is the only factor that determines the screening properties of ions, the identical reduction of the current induced by Ba^{2+} and Mg^{2+} at the low limit of divalent concentration (Fig. 8) is indicative of a charge screening effect. By contrast, data from rat muscle Na^+ channel indicate a negligible effect of surface charges on ion conduction (Ravindran et al., 1992). At low $[Na^+]$, this channel does not show rectification in the current–voltage relation and exhibits a drop in the conductance at the low limit of $[Na^+]$. These differences may be due to differences in the density of the surface charges present in these two channels.

Single ion occupancy yields to high heterogeneity in the estimation of K_{app} and σ

A second source of potential variation in the available estimates of the Na^+ channel surface charge density

TABLE 2 **Apparent dissociation constants (K_{app}), maximal conductance (γ_{max}), and vestibule surface charge (σ) for different Na^+ channels**

Channel	K_{app}	γ_{max}	σ	$[Na^+]$	Reference
	M	*pS*	$-e/nm^2$	*M*	
Eel electroplax	2.200	37	0.39	0.020–1.00	Recio-Pinto et al., 1987
Dog brain	1.500	45	0.38	0.020–3.50	Green et al., 1987
Squid giant axon	0.214	11	0.26	0.015–1.00	Correa et al., 1991
Lobster walking leg	0.101	19	0.08	0.015–1.00	Castillo et al., 1992
Rat brain	0.037	31	—	0.025–1.00	French et al., 1986
Squid optic nerve	0.011	23	—	0.005–0.54	Behrens et al., 1989
Rat skeletal muscle	0.007	21	—	0.003–0.48	Moczydlowski et al., 1984
Low $[Na^+]$					
γ_1	0.028 ± 0.004	17.0 ± 0.5	0.034 ± 0.003	0.0004–0.50	Present work
γ_2	0.029 ± 0.002	12.3 ± 1.3	0.033 ± 0.002	0.0004–0.50	Present work
Rat skeletal muscle	0.031 ± 0.005	22.3 ± 3.0	0.021 ± 0.002	0.0005–0.50	Ravindran et al., 1992
High $[Na^+]$					
γ_1	1.270 ± 0.230	36.0 ± 3.0	0.210 ± 0.022	0.0100–3.00	Present work
γ_2	1.820 ± 0.500	29.0 ± 1.4	0.220 ± 0.022	0.0100–3.00	Present work
Rat skeletal muscle	1.450 ± 0.002	38.8 ± 5.0	0.240 ± 0.002	0.0100–3.00	Ravindran et al., 1992

For the squid Na^+ channel, K_{app} was obtained from the depth of the energy wells of the barrier model proposed by Correa et al. (1991). Data from eel electroplax Na^+ channel were obtained by us from the Recio-Pinto et al. (1987) γ versus $[Na^+]$ relation. Data are means ± SD of the estimations. (—) The authors did not consider surface charge effects in their calculations. All fits assume single-ion channel behavior.

arises from the ion occupancy model used to fit the data (see Table 1). When single-ion occupancy has been assumed, large variations in K_{app} as well as the surface charge estimation have been observed (Table 2). Values for K_{app} ranging from 7 to 2,200 mM have been obtained, with higher charge densities being associated with larger values for K_{app}. Such variability in the values for the dissociation constant and σ would not be expected for the Na^+ channels types cloned thus far. The high homology existing for the pore-forming region of different Na^+ channel types suggests that the interaction between Na^+ and the pore is a conserved feature among Na^+ channels (Guy and Conti, 1990). Thus, the observed variability in K_{app} for different Na^+ channels may not be indicative of actual differences in the energy of interaction between Na^+ and the channel pore. Instead, it may represent the application of a simplified single-ion model whose ability to fit the conductance versus $[Na^+]$ data depends on the range of $[Na^+]$ studied (Table 2). Thus, in those cases in which this relation has been obtained in a range displaced toward low $[Na^+]$, the values for K_{app} were low and, conversely, large values for K_{app} were obtained when the range was displaced toward higher $[Na^+]$. To further test this idea and to stress the importancy of the data collected at $[Na^+] > 500$ mM and < 10 mM, we used a single-ion model incorporating surface charge effects (Green et al., 1987; Castillo et al., 1992) to fit Ravindran et al. (1992) data and ours over two widely overlapping $[Na^+]$ ranges: a range including all experimental points obtained <500 mM Na^+ (0.4–500 mM; low $[Na^+]$ range) and a second range including all experimental points >10 mM (10–3,000 mM; high $[Na^+]$ range). The fit of the data over these two $[Na^+]$ ranges yielded quite different values for K_{app} and σ and agreed with previously published estimates for other Na^+ channels (Table 2, see above). The obtained values for K_{app} and σ at the high concentration range approached values very similar to those obtained by Green et al. (1987), whereas at the low concentration range they approached the values obtained by Behrens et al. (1989) and Moczydlowski et al. (1984). Thus, the observed wide range of K_{app} estimates between different Na^+ channels may not be due to structural disparity in the permeation structure that interacts intimately with Na^+, but, rather, it is result of the application of single-ion occupancy models to describe a multiion channel under very different ranges of $[Na^+]$.

Multiion models reduce heterogeneity in the estimation of K_{app} and σ

For the sake of comparison, let us assume that all BTX-modified Na^+ channels are two-site, multiion channels. Let us further assume that the differences between Na^+ channels reside in the surface charge density present in the vestibules. If this is the case, then it is possible to fit the conductance versus $[Na^+]$ data for all BTX-modified Na^+ channels with quite similar values for K_{app} (Table 3). We kept constant the energy wells (−4.0 kT [18 mM]) and the electrostatic repulsion factor. The only adjustable parameters were σ and the energy barriers. The standard deviations of the estimates are quite small, indicating that the fit is very good for all the channels considered. The only data set that did not provide a reasonably good fit was rat brain sodium channel (French et al., 1986). Fitting these data required us to make the energy wells an adjustable parameter also (see Table 3). In conclusion, determinations of the surface charge density from conductance–permeant ion concentration relations depend on the degree of occupancy of the model used to describe the data.

TABLE 3 **Energy parameters for the charged-vestibules-3B2S model for different BTX-modified Na^+ channels**

Channel	Peaks	σ	Reference
	kT	$-e/nm^2$	
Squid giant axon	10.06 ± 0.04	0.266 ± 0.024	Correa et al., 1991
Eel electroplax	9.08 ± 0.02	0.230 ± 0.014	Recio-Pinto et al., 1987
Dog brain	8.92 ± 0.01	0.157 ± 0.035	Green et al., 1987
Rat skeletal muscle	8.89 ± 0.03	0.020 ± 0.001	Moczydlowsky et al., 1984
Rat skeletal muscle	8.93 ± 0.03	0.009 ± 0.001	Ravindran et al., 1992
Squid optic nerve	8.76 ± 0.03	0.006 ± 0.006	Behrens et al., 1989
Rat brain	9.36 ± 0.05	0.003 ± 0.001	French et al., 1986
Lobster walking leg	9.17 ± 0.01	0.004 ± 0.001	Castillo et al., 1992

The fit to the γ versus $[Na^+]$ data was done using an energy barrier model similar to that shown in Fig. 6. Only the peak energies and the surface charge density were let to vary; the well depth and the repulsion factor were kept constant. With the expression $K_{app} = \exp(-\text{Energy}_{well}/kT)$, we fix K_{app} in 18 mM in all cases by setting Energy_{well} to −4.0 kT. This fitting procedure was successful in all cases except data from French et al. (1986) and Ravindran et al. (1992). For data from French et al. (1986), we also let vary the well depth, and the best fit was obtained with wells of −3.1 kT, giving K_{app} = 45 mM. For data from Ravindran et al. (1992), in the extreme low concentration range the theoretical values were consistently higher than experimental values. Data are mean ± SD of the estimations.

A planar geometry of the charged surface

In the lack of structural information regarding the exact location of the charges involved in the process of ion conduction, we have used the Gouy–Chapman theory to extract the surface charge density in the channel mouths. For an ion channel protein, the main caveat of this simplified model is the assumption that the protein–water interface constitutes a plane of homogeneously distributed surface charge. Dani (1986) and Cai and Jordan (1990) have attempted to deal with more realistic charge distributions in the vestibules by solving numerically the nonlinear Poisson–Boltzmann equation. Contrary to the Gouy–Chapman theory prediction, the numerical solutions for point charges located in the vestibules indicates that the conductance should approach zero as the $[Na^+]$ is reduced to zero. Using this theory, Cai and Jordan (1990) fitted the data of Green et al. (1987) obtained over the $[Na^+]$ range of 20 mM to 3.5 M. They concluded that the pore must have an hour-glass shape and the charges must be located near the constriction entrance to explain Green et al. (1987) data. For this particular geometry of charge distribution, $[Na^+]$ in the vestibule and hence channel conductance should start falling off abruptly at $[Na^+]$ <100 mM. However, our results for γ_1 and γ_2 obtained over a wider $[Na^+]$ range clearly indicate a small variation of the conductance in the 0.4–10 mM $[Na^+]$ range (Fig. 6, *A* and *B*) and that the fitting to Gouy–Chapman theory is reasonable. Consequently, our data suggest a more planar geometry for charge distribution than that proposed by Cai and Jordan (1990) for the BTX-modified Na^+ channel from dog brain.

It is important to note that because the surface potential does not approach to $-\infty$ as bulk $[Na^+]$ approaches to zero, the Gouy–Chapman theory should break down at sufficiently low ionic strength. Cai and Jordan (1990) have proposed that this breakdown occurs when the Debye length is larger than the radius of the circumference over which the fixed charge is spread. The range of bulk $[Na^+]$ at which the ion concentration at the channel entrances is predicted to approach zero is a function of both the fixed charge density and their geometrical distribution. The charge density estimation is model dependent (Tables 1–3) and the geometrical distribution unknown.

The Stokes radius for the sodium channel is 9.5 nm (Agnew et al., 1978). Assuming that this figure represents the radius of the channel protein in which the negative charges are spread and according to Cai and Jordan (1990), at $[Na^+]$ = 1 mM, when the Debye length is 9.6 nm, the conductance should start to fall toward zero. This is the lower theoretical limit at which $[Na^+]$ should start dropping. Our data show a small reduction of the conductance at $[Na^+]$ <1 mM (Fig. 6, *A* and *B*); however, to study conduction at bulk $[Na^+]$ <400 μM becomes technically difficult. The low pH buffer concentration needed to achieve lower $[Na^+]$ renders pH hard to control. Also, as surface potential increases with the reduction of the ionic strength, $[H^+]$, as well as $[Na^+]$, is increased in the vestibules, whereas the anionic concentration ($MOPS^-$) is decreased.[2] Thus, the local pH may change in an unknown manner, making results obtained at very low ionic strength difficult to interpret.

[2] As a result of the fixed charges located in the channel entrances, the $[H^+]$, as well as every other cation concentration, is increased. When the $[Na^+]$ is 0.4 mM, the proton concentration in the channel vestibules is ~10-fold larger than in the bulk. Since we do not know at present the *pK*s of the charged groups in the vestibules, it is not possible to calculate in which amount the fixed charge density is underestimated. However, there is good evidence for the existence of a glutamic acid residue in the external vestibule (Noda et al., 1989). If this residue has the same p*K* as glutamic acid (4.7), a decrease in the external pH from 7 to 6 should not affect greatly the ionization state of this residue.

We thank Dr. John Daly for the gift of batrachotoxin. Special thanks to Dr. O. Alvarez for his unending patience in teaching us how to work with energy barrier models and Dr. P. Brehm for critical reading of this manuscript. The generosity of Drs. E. Moczydlowski and Recio-Pinto for sharing data previous publication on BTX-modified channels is cheerfully acknowledged.

This work was supported by National Institutes of Health grant GM-35981, Fondo Nacional de Investigacion grants 451-1988 and 863-1991, and a grant from the Tinker Foundation. R. Latorre is recipient of a John D. Guggenheim fellowship and he thanks the Dreyfus Bank for generous support from a private foundation they made available to him.

Received for publication 21 September 1992 and in final form 30 November 1992.

REFERENCES

Agnew, W. S., S. R. Levinson, J. S. Brabson, and M. A. Raftery. 1978. Purification of the tetrodotoxin-binding component associated with the voltage-sensitive sodium channel from *Electrophorus electricus* electroplax membranes. *Proc. Natl. Acad. Sci. USA.* 76:2606–2610.

Alvarez, O., A. Villarroel, and G. Eisenman. 1992. A general procedure to calculate ion currents from energy profiles in a three-barrier two-site channel model. *Methods Enzymol.* 207:816–854.

Begenisich, T., and M. D. Cahalan. 1980*a*. Sodium channel permeation in squid axons. I. Reversal potential experiments. *J. Physiol. (Lond.).* 307:217–242.

Begenisich, T., and M. D. Cahalan. 1980*b*. Sodium channel permeation in squid axons. II. Non-independence and current-voltage relations. *J. Physiol. (Lond.).* 307:243–257.

Behrens, M. I., A. Oberhauser, F. Bezanilla, and R. Latorre. 1989. Batrachotoxin-modified sodium channels from squid optic nerve in planar bilayers. Ion conduction and gating properties. *J. Gen. Physiol.* 93:23–41.

Cachelin, A. B., J. E. Peyer, S. Kokubun, and H. Reuter. 1983. Sodium channels in cultured cardiac cells. *J. Physiol. (Lond.).* 340:389–401.

Cai, M., and P. Jordan. 1990. How does vestibule surface charge affect ion conduction and toxin binding in a sodium channel. *Biophys. J.* 57:883–891.

Castillo, C., R. Villegas, and E. Recio-Pinto. 1992. Alkaloid-modified sodium channels from lobster walking leg nerves in planar lipid bilayers. *J. Gen. Physiol.* 99:897–930.

Cecchi, X., O. Alvarez, and D. Wolff. 1986. Characterization of a calcium-activated potassium channel from rabbit intestinal smooth muscle incorporated into planar bilayers. *J. Membr. Biol.* 91:11–18.

Correa, A. M., R. Latorre, and F. Bezanilla. 1991. Ion permeation in normal and batrachotoxin-modified Na^+ channels in the squid giant axon. *J. Gen. Physiol.* 97:605–625.

Dani, J. 1986. Ion-channel entrances influences permeation. Net charge, size, shape and binding considerations. *Biophys. J.* 49:607–618.

Dani, J., and G. Eisenman. 1987. Monovalent and divalent cation permeation in acetylcholine receptor channels. Ion transport related to structure. *J. Gen. Physiol.* 89:959–983.

Fox, J. A. 1987. Ion channel subconductance states. *J. Membr. Biol.* 97:1–8.

French, R. J., B. K. Krueger, and J. F. Worley. 1986. From brain to bilayer. Sodium channels from rat neurons incorporated into planar lipid membranes. *In* Ionic Channels in Cells and Model Systems. R. Latorre, editor. Plenum Publishing Corp., New York. 273–290.

Garber, S., and C. Miller. 1987. Single Na^+ channels activated by veratridine and batrachotoxin. *J. Gen. Physiol.* 89:459–480.

Grahame, D. C. 1947. The electrical double layer and the theory of electrocapillarity. *Chem. Rev.* 41:441–501.

Green, W. N., L. B. Weiss, and O. S. Andersen. 1987. Batrachotoxin-modified sodium channels in lipid bilayers. Ion permeation and block. *J. Gen. Physiol.* 89:841–872.

Guy, H. R., and F. Conti. 1990. Pursuing the structure and function of voltage gated channel. *Trends Neurosci.* 13:201–206.

Hidalgo, C., C. Parra, G. Riquelme, and E. Jaimovich. 1986. Transverse tubules from frog skeletal muscle: purification and properties of vesicles sealed with the inside-out orientation. *Biochim. Biophys. Acta.* 855:79–88.

Hille, B., and W. Schwarz. 1978. Potassium channels in excitable cells as multi-ion single-file pores. *J. Gen. Physiol.* 72:409–442.

Khodorov, B. I. 1985. Batrachotoxin as a tool to study voltage sensitive sodium channels of excitable membranes. *Prog. Biophys. Mol. Biol.* 45:57–148.

Krueger, B. K., J. F. Worley, and R. French. 1983. Single sodium channels from rat brain incorporated into planar lipid bilayer membranes. *Nature (Lond.).* 303:172–175.

Latorre, R. (ed.). 1986. Ion channels in cells and in model systems. Plenum Press, New York. 437 pp.

Latorre, R., P. Labarca, and D. Naranjo. 1992. Surface charge effects on ion conduction in ion channels. *Methods Enzymol.* 207:471–501.

Levinson, R., W. Thornhill, D. Duch, E. Recio-Pinto, and E. Urban. 1990. The role of nonprotein domains in the function and synthesis of voltage-gated sodium channels. *In* Ion Channels. Vol. 2. T. Narahashi, editor. Plenum Publishing Corp., New York. 33–63.

MacKinnon, R., R. Latorre, and C. Miller. 1989. Role of surface electrostatics in the operation of a high-conductance Ca^{2+}-activated K^+ channel. *Biochemistry.* 28:8092–8099.

Matsuda, H., H. Matsuura, and A. Noma. 1989. Triple-barrel structure of inwardly rectifying potassium channel revealed by Cs^+ and Rb^+ block in guinea-pig heart cells. *J. Physiol. (Lond.).* 413:139–157.

McLaughlin, S. 1977. Electrostatic potentials at the membrane-solution interfaces. *Curr. Top. Membr. Transp.* 9:71–144.

McLaughlin, S. 1989. The electrostatic properties of membranes. *Annu. Rev. Biophys. Biophys. Chem.* 18:113–136.

Meves, H., and K. Nagy. 1989. Multiple conductance states of sodium channel and of other ion channels. *Biochim. Biophys. Acta.* 988:99–195.

Miller, C. 1982. Open-state substructure of single chloride channel from *Torpedo electroplax*. *Philos. Trans. R. Soc. B.* 299:401–411.

Miller, C. (ed.). 1986. Ion channels reconstitution. Plenum Press, New York, 577 pp.

Moczydlowski, E., S. Garber, and C. Miller. 1984. Batrachotoxin-activated sodium channels in planar lipid bilayers: competition of tetrodotoxin block by Na. *J. Gen. Physiol.* 84:665–686.

Naranjo, D., O. Alvarez, and R. Latorre. 1989. Ion conduction characteristics of batrachotoxin-modified sodium channels from frog muscle. *Biophys. J.* 55:402*a*. (Abstr.).

Naranjo, D., O. Alvarez, and R. Latorre. 1990. Ion conduction and kinetic properties of batrachotoxin-modified sodium channels from frog muscle. *Biophys. J.* 57:109*a*. (Abstr.).

Nilius, B., J. Vereecke, and E. Carmeliet. 1989. Different conductance states of the bursting Na channel in guinea-pig ventricular myocytes. *Pfluegers Arch.* 413:242–248.

Noda, M., H. Suzuki, S. Numa, and W. Stuhmer. 1989. A single point mutation confers tetrodotoxin sensitivity and tetrodotoxin insensitivity on the sodium channel. II. *FEBS (Fed. Eur. Biochem. Soc.) Lett.* 259:213–216.

Patlak, J. 1988. Sodium channel subconductance levels measured with a new variance-mean analysis. *J. Gen. Physiol.* 92:413–430.

Ravindran, A., H. L. Kwiecinski, O. Alvarez, G. Eisenman, and E. Moczydlowski. 1992. Modeling ion permeation through batrachotoxin-modified Na^+ channels from rat skeletal muscle with a multi-ion pore. *Biophys. J.* 61:494–508.

Ravindran, A., L. Schild, and E. Moczydlowski. 1991. Divalent cation selectivity for external block of voltage dependent Na^+ channels prolonged by batrachotoxin. Zn^{2+} induces discrete substates in cardiac Na^+ channels. *J. Gen. Physiol.* 97:89–115.

Recio-Pinto, E., D. S. Duch, S. R. Levinson, and R. W. Urban. 1987. Purified and unpurified sodium channels from the eel electroplax in planar lipid bilayers. *J. Gen. Physiol.* 90:375–395.

Schild, L., A. Ravindran, and E. Moczydlowski. 1991. Zn^{2+}-induced subconductance events in cardiac Na^+ channels prolonged by batrachotoxin. Current-voltage behavior and single channel kinetics. *J. Gen. Physiol.* 97:117–142.

Schreibmayer, W., H. Tritthart, and H. Schindler. 1989. The cardiac sodium channel shows a regular substate pattern indicating synchronized activity of several ion pathways instead of one. *Biochim. Biophys. Acta.* 988:99–105.

Smith-Maxwell, C., and T. Begenisich. 1987. Guanidinium analogues as probes of the squid axon sodium pore. Evidence for internal surface charges. *J. Gen. Physiol.* 90:361–364.

Villarroel, A. 1989. Mechanism of ion conduction in the large calcium-activated potassium channel. Ph.D. dissertation. University of California, Los Angeles. 133 pp.